Antifouling pseudo-zwitterionic poly(vinylidene fluoride) membranes with efficient mixed-charge surface grafting via glow dielectric barrier discharge plasma-induced copolymerization

Antoine Venault, Ta-Chin Wei, Hsiao-Lin Shih, Chin-Cheng Yeh, Arunachalam Chinnathambi, Sulaiman Ali Alharbi, Séverine Carretier, Pierre Aimar, Juin-Yih Lai, Yung Chang

Antifouling pseudo-zwitterionic poly(vinylidene fluoride) membranes with efficient mixed-charge surface grafting via glow dielectric barrier discharge plasma-induced copolymerization

Antoine Venault [a], Ta-Chin Wei [a,*], Hsiao-Lin Shih [a], Chin-Cheng Yeh [a], Arunachalam Chinnathambi [b], Sulaiman Ali Alharbi [b], Séverine Carretier [a], Pierre Aimar [c], Juin-Yih Lai [a], Yung Chang [a,b,**]

[a] R&D Center for Membrane Technology and Department of Chemical Engineering, Chung Yuan Christian University, Chung-Li, Taoyuan 32023, Taiwan
[b] Department of Botany and Microbiology, College of Science, King Saud University, P.O. Box 2455, Riyadh 11451, Saudi Arabia
[c] Laboratoire de Génie Chimique, Université Paul Sabatier, 118 route de Narbonne, 31062 Toulouse Cedex 9, France

Keywords:
Pseudo-zwitterionic
Mixed-charge
PVDF membrane
GDBD plasma
Antifouling

A B S T R A C T

This work reports on the glow dielectric barrier discharge (GDBD) plasma-induced surface grafting of poly(vinylidene fluoride) (PVDF) membranes with mixed-charge copolymers of [2-(methacryloyloxy) ethyl] trimethylammonium (TMA) and sulfopropyl methacrylate (SA). The aim is to investigate the antifouling properties and the hemocompatibility of this system. We first characterize the physico-chemical properties of the membranes. With SA alone in the coating solution, efficient grafting cannot be achieved as monomer is blown away during grafting. Membranes grafted with a mixture of SA and TMA, or TMA alone do not meet this problem and grafting density ranged between 0.29 and 0.41 mg/cm^2. Bovine-serum-albumin and lysozyme adsorption tests (70% reduction) and *Escherichia coli* attachment test (annihilation of adhesion) unveil that pseudo-zwitterionic PVDF membranes are very efficient to reduce biofouling in static condition. Different fouling resistance behaviors are observed in dynamic conditions. Permeability of virgin membranes progressively decreases over the cycles, arising from a gradual pore blockage and irreversible fouling. All potential adsorption sites of pseudo-zwitterionic membrane and membrane with positive charge-bias are fouled after the first cycle, and flux recovery is maximal in the following cycles. This behavior is ascribed to the lack of homogeneity of the surface grafting. Finally, pseudo-zwitterionic membranes are hemocompatible (resistance to blood cells, low hemolysis activity). Provided a better tuning of surface uniformity, the method and system presented in this work are a promising approach to the new generation of antifouling mixed-charge membranes for water treatment or blood contacting devices.

1. Introduction

In order to address the issue of biofouling of hydrophobic porous membranes, three main research directions are currently under investigation. In-situ modification consists in blending the hydrophobic polymer with an appropriate amphiphilic copolymer in a common solvent, before inducing phase inversion of the polymeric system [1–4]. This method is direct (formation and modification all at once) but can lead to major changes of the membrane structure, and so to modifications of arising properties, which may not be on target. A second approach gathers self-assembling or coating methods [5,6]. Even though numerous variations of the process exist, hydrophobic interactions between the matrix polymer and the hydrophobic moieties of the surface-modifier are always established, providing the membrane with antifouling properties. In this approach, stability can be questioned. Finally, the third approach is also a surface modification process, but this time, the modifier is chemically bonded to the membranes [7–9]. This later approach permits to readily prepare antifouling stable membranes at laboratory scale with controlled surface properties.

If PEGylated-derivatives polymers have been widely studied and proven to provide hydrophobic membranes with low-biofouling properties [10–12], zwitterionic polymers, more stable, are becoming predominant antifouling materials [13–15]. All these

* Corresponding author.
** Corresponding author at: R&D Center for Membrane Technology and Department of Chemical Engineering, Chung Yuan Christian University, Chung-Li, Taoyuan 32023, Taiwan.
E-mail addresses: tcwei@cycu.edu.tw (T.-C. Wei), ychang@cycu.edu.tw (Y. Chang).

materials satisfy the criteria for ideal antifouling material earlier defined by Whitesides and coworkers [16], and reminded here: (1) electroneutrality should be ensured; (2) the material should not possess H-bond donors; (3) the material should have H-bond acceptors and (4) it should contain polar functional groups. A new class of materials may satisfy these criteria: the so-called mixed-charge polymers [17–22]. These systems are composed of both electronegative and electropositive moieties, and mimic zwitterionic polymers. However, as reminded by Edwards and coworkers, mixed-charge polymers functionality are not impacted by the introduction of other functional groups [22]. In other words, they are even more stable than zwitterionic materials. These systems have mostly been tested to form antifouling hydrogels or to modify model dense surfaces. Besides their numerous advantages listed by Prof. Jiang's group such as the simplicity of synthesis, the ease of applicability, the numerous potential raw materials as well as the availability of functional groups [18], these systems allow to investigate the effect of charge bias on protein, bacteria or cell adhesion [23]. This aspect can be of interest for fundamental comprehension of mechanisms at play responsible for biofouling.

Yet to the best of our knowledge, only one previous study mentioned the surface modification of polypropylene membranes by mixed-charge polymer [24]. The use of mixed-charges has never been tested using PVDF as a matrix material, very common in membrane commercial applications. Results of such an investigation could be of major interests for the application of membranes in water treatment or blood filtration, two major fields in which in-depth investigations are still required to efficiently mitigate biofouling. This lack of research work suggested the need for a dedicated study. Here, we modified poly(vinylidene fluoride) (PVDF) commercial microfiltration membranes using mixed-charges of [2-(methacryloyloxy)ethyl] trimethylammonium (TMA) and 3-sulfopropyl methacrylate (SA). After monomer coating, we applied a new process of glow dielectric barrier discharge (GDBD) plasma treatment to the membranes. Our strategy, schemed in Fig. 1, consists first in fully characterizing the physico-chemical properties of membranes and evaluating the degree of control of the overall process, through the determination of charge bias. Then, we move onto the characterization of potential antifouling and hemocompatible properties of modified membranes in static conditions (adsorption of proteins, bacteria and blood cells) and dynamic conditions (filtration). Eventually, this research work sheds light on the promising use of mixed-charge as alternate surface-modification agents for PVDF microfiltration membranes.

2. Experimental

2.1. Materials

PVDF microporous membranes (diameter: 47 mm; pore size: 0.1 μm; porosity: 70%; thickness: 125 μm) were purchased from Millipore®. 2-(Methacryloyloxy) ethyl]trimethylammonium chloride (TMA) and 3-sulfopropyl methacrylate potassium salt (SA) were bought from Sigma Chemical Co. Solvent used, isopropanol, was obtained from Aldrich. A Millipore water purification system permitted to prepare deionized water with a minimum resistivity of 18.0 MΩ cm.

2.2. Methods

2.2.1. Surface modification of PVDF membranes

TMA and SA were first dissolved in an isopropyl alcohol/water (1:1) mixture of solvents at controlled molar ratio as defined in Table 1. Then, commercial PVDF membranes (Merck Millipore VVHP04700) were spray-coated by the monomer solutions. After TMA/SA monomer coating (set at 3 mg/cm^2), membranes were placed inside an atmospheric-pressure GDBD plasma to induce graft-polymerization. The plasma reactor consists of two quartz plates of 10 cm in width, covered with copper electrodes of 7 cm in width. Helium plasma of 30 slm flowrate was generated by 13.56 MHz RF power (Cesar 136, Dressler) of 100 W. The treatment time was 60 s. After plasma induced grafting, PVDF membranes were extracted with isopropanol for 90 min in the ultrasonic device to strip off homopolymers and unreacted monomers. Finally, membranes were dried for 24 h in a vacuum oven under reduced pressure to remove residual solvent.

2.2.2. Physicochemical characterization of membranes

The grafting density of mixed-charge moieties onto PVDF membranes was evaluated from weight measurements: membranes were weighed before and after surface modification. The difference in weight per unit surface area was taken to be the grafting density. The accuracy of this evaluation will be further

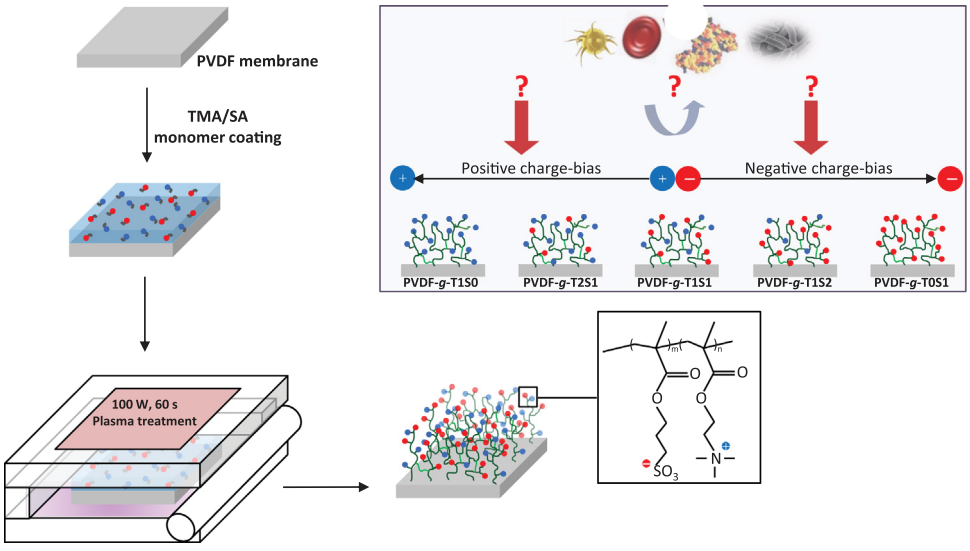

Fig. 1. Scheme of research concept of this investigation. Virgin PVDF membranes are coated with TMA and SA monomers, before undergoing plasma polymerization. By carefully choosing the initial monomer ratio, the final surface charge can be controlled. Therefore, it should be possible to regulate the interactions with biofoulants from waters or blood – proteins, bacteria, blood cells, and lead to a low-biofouling surface.

Table 1
Preparation and characterization of virgin and surface-modified PVDF membranes using TMA and SA.

Sample ID	Grafting conditions			Characterization of membranes[a]			
	TMA (mol%)	SA (mol%)	TMA/SA	TMA/SA (ϕ_1)	TMA/SA (ϕ_2)	Grafting density (mg/cm^2)	Zeta-potential at pH 7.4 (mV)
PVDF	0	0	–	/	/	0	4.7 ± 0.8
PVDF-*g*-T1S0	100	0	100/0	/	/	0.32 ± 0.02	22.7 ± 2.7
PVDF-*g*-T2S1	67	33	2/1	1.5	1.29	0.41 ± 0.03	15.2 ± 2.4
PVDF-*g*-T1S1	50	50	1/1	1.09	1.01	0.36 ± 0.02	0.6 ± 5.2
PVDF-*g*-T1S2	33	67	1/2	0.76	0.87	0.29 ± 0.01	-3.4 ± 0.5
PVDF-*g*-T0S1	0	100	0/100	0	0	0.02 ± 0.01	-8.4 ± 1.2

[a] ϕ_1 and ϕ_2 were obtained by ATR-FTIR and XPS characterization, respectively.

discussed in Section 3. Note that 3 independent tests were performed for each surface-modification condition, and the average is reported in this work. The surface of virgin and grafted membranes was observed by scanning electron microscope, with a Hitachi S-3000 instrument operated at an accelerating voltage of 15 keV. Before observation, all samples were sputter-coated with gold for 150 s. Membranes were also examined by atomic force microscope. A JPK Instruments AG multimode equipped with a NanoWizard scanner was used, and was operated in air tapping mode. Images were acquired with a commercial Si cantilever, having a resonant frequency of 320 kHz. The relative humidity was less than 40%. The surface chemistry of membranes was characterized by FT-IR and XPS. A Perkin-Elmer Spectrum One spectrophotometer operating with a ZnSe internal reflection element was employed to carry out FT-IR characterization. Spectra were all captured at a resolution of 4 cm^{-1}, and by averaging 32 scans. X-ray photoelectron spectroscopy analysis was performed with a Thermo Scientific K-Alpha using a monochromated Al Kα X-ray source (1486 eV) at a take-off angle of 90°. Further details regarding the operating procedures and settings are provided elsewhere [24]. To evaluate the zeta potential of membranes at pH 7, samples (length: 2 cm; width 1 cm) were placed on the adjustable cell of a SurPASS instrument. A phosphate buffer solution was prepared (salt concentration: 0.16 M), and used to infiltrate the instrument and the membranes. Then the surface zeta potential of the virgin and the grafted PVDF membranes could be measured.

2.2.3. Evaluation of hydration properties of membranes

10 Independent measurements of water contact angle were performed on each membrane, using an automatic water contact angle meter bought from Kyowa Interface Science Co. (Model CA-VP). All measurements were done at ambient temperature (about 25 °C). The hydration capacity of the membranes was evaluated by immersing membrane samples with a diameter of 1.3 cm into water for 24 h. Afterwards, superficial water was gently wiped out of the surfaces, and membranes weighed. The differential per unit surface area of the sample between the wet weight and the dry weight was taken to be the hydration capacity of the membrane tested. For each membrane, 5 independent tests were done.

2.2.4. Evaluation of protein adsorption and bacterial attachment onto membranes

Two model proteins were tested at first: bovine-serum-albumin (BSA, molecular weight: 66,000 g mol^{-1}, Sigma) and lysozyme (LY, molecular weight: 14,300 g mol^{-1}, Sigma). The adsorption tests of BSA and LY were performed at 25 °C according to the following experimental protocol. Membrane samples (diameter: 1.3 cm) were positioned in a 24-well plate. 1 mL of pure ethanol was then added to each individual well. Incubation of samples with alcohol lasted 30 min, and aimed at swelling the samples, and promoting diffusion and subsequent adsorption of proteins. Then, alcohol was removed and replaced by phosphate-buffered saline (PBS). Immersion of samples in PBS lasted 2 h, after which, 1 mL of either BSA or LY was added to the wells, and incubated with membranes for another 2 h. Eventually, the absorbance of the liquid solution in contact with the membrane samples was measured at 280 nm, using a Biotech UV-Visible spectrophotometer (model: PowerWave XS), which permitted to assess the remaining concentration of BSA or LY, and so the total amount of proteins that was adsorbed by the virgin and surface-modified membranes. The values reported correspond to the average of three independent measurements.

Bacterial attachment was conducted according to the following procedure. *Escherichia coli* bacteria were cultivated at 37 °C and 100 rpm in a solution containing 5.0 mg/mL peptone and 3.0 mg/mL beef extract. Once the stationary phase reached after 12 h (corresponding to a cell concentration of about 10^8 cell/mL), membrane samples, pre-washed several times with PBS and placed in individual wells of a 24-well plate, were incubated with 1 mL of bacterial solution for 3 h. Thereafter, bacterial solution was removed and membrane samples thoroughly washed with PBS. 200 μL of Live/Dead Baclight were used to stain bacterial adhering to the samples, and staining was performed for 5 min. Membranes were washed again 5 times using PBS, and samples observed by confocal microscopy (LSCM, A1R, Nikon, Japan) to evaluate the extent of micro-biofouling by bacteria. All images were taken at $\lambda_{ex}=488$ nm/$\lambda_{em}=520$ nm. Also, in the present study, we only focus on live bacteria.

2.2.5. Resistance to biofouling during filtration

Resistance to biofouling during filtration was assessed with a dead-end cell filtration system. The stainless steel filtration cell used has a diameter of 54 mm. The actual filtration area was 8.04 cm^2. The cell was connected to a nitrogen compression cylinder. PVDF and selected grafted PVDF membranes were immersed in ethanol for 0.5 h. Then, the membrane considered for the test was placed in the cell, and an overpressure cycle was run for 0.5 h at ambient temperature, 1.5 atm and using DI water. Afterwards, the pressure was reduced to 1 atm, and water flux recorded for another 30 min. Then, filtration cell was connected to a tank containing BSA protein at 1 g/L, and BSA cycle was run for about 2 h. After BSA cycle, the membrane was washed by flushing it was DI water and immersing it in DI water for 10 min. Then, the operation was repeated. In total, after the assessment of initial water permeability, 3 BSA-water cycles were run. Flux recovery ratio (FRR), reversible flux decline ratio (DRr) and irreversible flux decline ratio (DRi) were calculated using equations reminded in the related section.

2.2.6. Evaluation of hemocompatibility of membranes

The hemocompatibility of membranes was evaluated through adsorption test of fibrinogen (FN, molecular weight: >300 kDa, Sigma), adhesion tests of thrombocytes and erythrocytes, as well by determining the hemolytic activity of virgin and surface

modified membranes. The adsorption test of FN was carried out according to the ELISA method reported elsewhere [25]. The adhesion of thrombocytes was studied as follows: platelets-rich-plasma (PRP) solution was obtained by centrifuging blood of a healthy volunteer for 10 min at 1200 rpm. This way, PRP could be easily separated from the other blood constituent. PVDF and grafted PVDF membrane samples having a 0.4 cm^2 surface area were positioned in a 24-well plate. After equilibrating each sample with phosphate buffered solution (PBS) for 2 h at ambient temperature, 200 μL of PRP solution were poured onto the membranes. Membranes were incubated with PRP solution for 2 h, at 37 °C. Then, PRP solution was removed, and membranes rinsed twice with 1 mL of PBS. Thereafter, a fixing solution, made of 2.5% (v/v) glutaraldehyde in PBS, was applied to the samples. Fixing step was run at 4 °C for 2 days. Finally, membranes were thoroughly washed with PBS and dehydrated with a graded ethanol series from PBS through 0–10–25–50–75–90–100% ethanol (v/v). Each dehydration step was run over 20 min. Samples could then be observed by confocal microscopy (LSCM, A1R, Nikon, Japan), at λ_{ex}=488 nm/λ_{em}=520 nm. The adhesion of erythrocytes was tested according to the following method. At first, red blood cell concentrate was obtained by centrifuging at 1200 rpm for 10 min 250 mL of blood from a human healthy volunteer. A volume V=200 μL of RBC concentrate was then incubated with membrane samples (0.4 cm^2) for 2 h at 37 °C. Afterwards, membranes were washed with PBS, and then immediately immersed in a glutaraldehyde solution (V=300 μL, 2.5% v/v in PBS). Incubation in fixing agent lasted 10 h and was performed at low temperature (4 °C). Eventually, membranes were rinsed several times with PBS, and observed by confocal microscopy with the same instrument and settings as those used to observe thrombocytes. Finally, hemolytic activity of membranes was also evaluated according to a procedure reported elsewhere [24].

3. Results and discussion

3.1. Surface grafting and physico-chemical characterizations

In this study, a series of TMA/SA surface modified PVDF membranes were prepared by GDBD plasma treatment. We first investigated the efficiency of surface grafting, through a number of physico-chemical characterizations. Results of grafting density displayed in Fig. 2, readily determined by weight measurements,

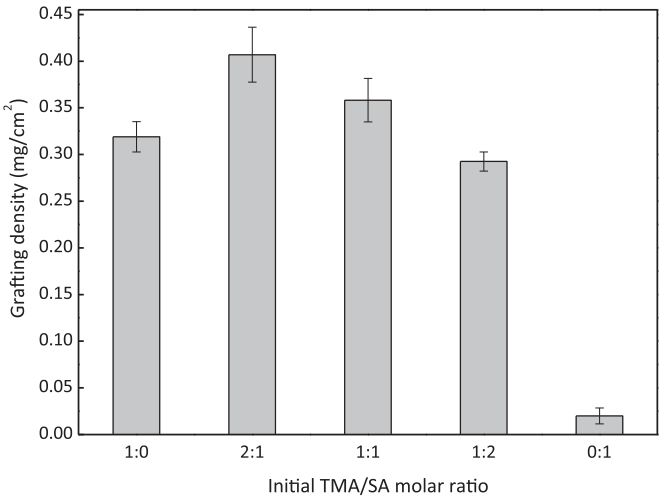

Fig. 2. Grafting density achieved after surface modification of commercial PVDF membranes by plasma treatment, as a function of the initial TMA/SA molar ratio in the coating bath.

indicate that the DBD plasma process is fairly well-controlled, as the error limits on data are small (< 0.03 mg/cm^2). However, several points can be discussed. First, if grafting density of all samples containing TMA groups – PVDF-*g*-T1S0, PVDF-*g*-T2S1, PVDF-*g*-T1S1 and PVDF-*g*-T1S2 – ranges between 0.3 and 0.4 mg/cm^2, that of PVDF-*g*-T0S1, only containing SA moieties is very small: 0.02 mg/cm^2. This is attributed to the fact that during plasma modification, solvent evaporation occured, leading to SA monomers precipitation. Under the action of flow rate, monomer particles were washed away, therefore preventing efficient grafting of the negative pendent groups on the surface. A few works dealing with chemical surface modification of PVDF membranes using zwitterionic or PEG moieties mention grafting density in the same range [14,15,26,27]. For instance, in the case of PVDF hollow-fiber membranes grafted with poly(2-hydroxyethylmethacry-late) and zwitterionic poly(3-(methacryloylamino)propyl-dimethyl-(3-sulfopropyl)ammonium hydroxide) polymer, Li et al. measured grafting density in the range 171–532 μg/cm^2 [26], which is in the same order of magnitude as those reported here. However, as monomers are different from those reported in literature, accurate comparisons cannot be done. In addition, the method to evaluate grafting density, in the present work or in literature, similar to that used to determine coating densities when self-assembling methods are used, can be criticized. As aforementioned, the method is based on difference of weight per unit surface of the membrane before and after modification. It implies that (i) monomers do not penetrate within the membrane and (ii) that the value for the surface area is known. Obviously, the first point cannot be warranted even if repulsive hydrophobic-hydrophilic interactions occur as hydrophobic porous membrane is used. If monomers have penetrated, than the actual surface grafting density reported is lower than the reported one. Also, the exact value of the surface area modified is unknown. Indeed, we considered the surface area of the sample which actually contains surface pores. Additionally, polymer chains at the surface of the membranes are probably not totally exposed to the monomers. Therefore, the actual surface must be lower, which would eventually lead to higher grafting density. In this respect, the trend obtained in this work (and others) should be considered first, rather than the actual values provided, because a number of approximations were done. It is also worth noting that from the SEM images presented in Fig. 3 as well as from the AFM characterization of Fig. S1, there does not seem to be important decreasing of surface porosity after surface modification, which would imply that permeation properties of the commercial PVDF membrane should be maintained in the MF range. It will have to be further checked in subsequent sections. Additionally, the surface roughness coefficient of membranes was maintained in a same range 140–200 nm. Therefore, from a physical point of view, the surface modification did not lead to important changes in the structure of the PVDF MF membrane.

Analysis of the surface chemistry can also indicate whether the monomers are efficiently grafted at the surface of the membranes. In this work we used both FT-IR (Fig. 4) and XPS (Fig. 5). As seen in Fig. 4, the FT-IR spectra of all membranes are very similar, but characteristic signals for the stretching bands of carboxyl groups (1730 cm^{-1}), sulfonate group (1038 cm^{-1}) and that of quaternary amine (947 cm^{-1}) can be seen, indicating the presence of mixed-charge brushes at the surfaces. Additionally, it was possible to determine the actual N/S ratio (and so the actual TMA/SA ratio) from the knowledge of the area of characteristic stretching bands (Table 1). XPS tests also ascertained the presence of TMA and SA moieties, and permitted to determine the actual TMA/SA content at the surface. From the N1s and S2p core level spectra presented in Fig. 5, the presence of sulfur (sulfonate groups, BE: 168.1 eV) and nitrogen (quaternary amine, BE: 402.3 eV) can be clearly evidenced [28,29]. A peak on N1s core level spectra was also observed

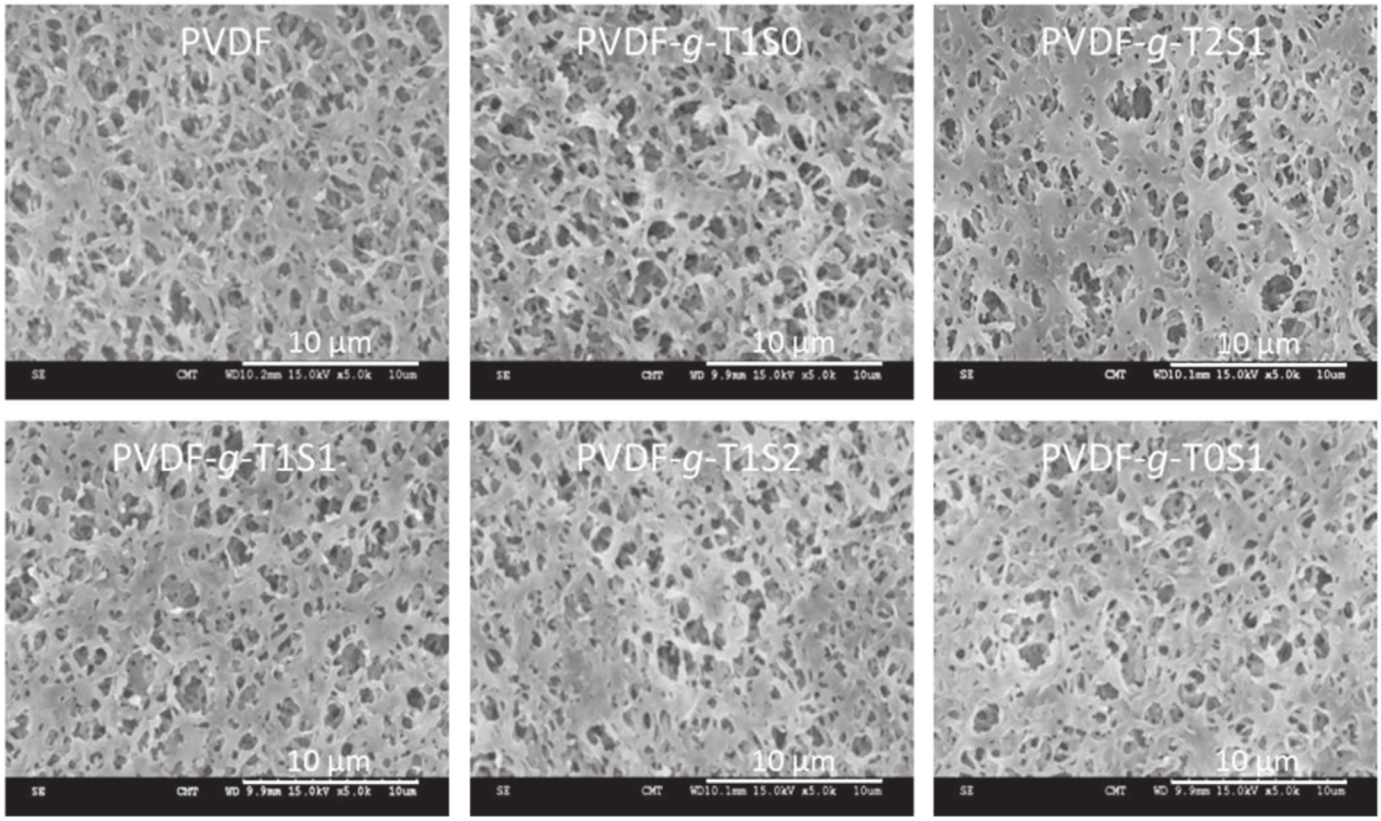

Fig. 3. Morphological observations of the virgin and surface-modified membranes' surface by SEM analysis.

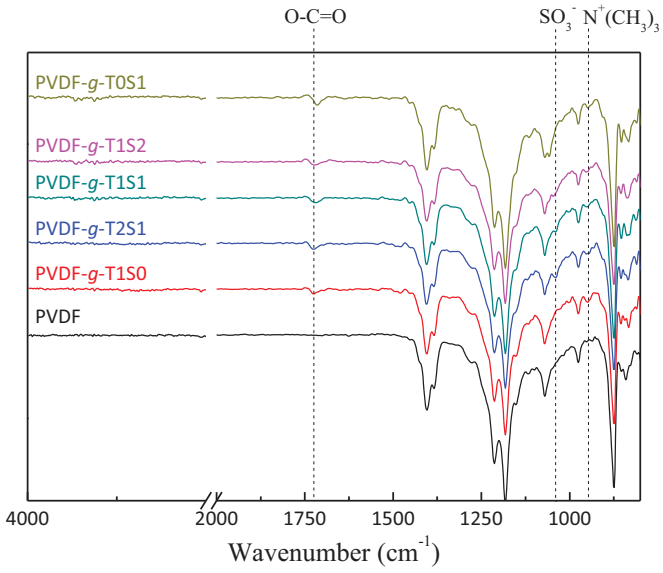

Fig. 4. FT-IR analysis of virgin and surface-modified membranes.

at about 399.5 eV, corresponding to tertiary amine group. The presence of these functional groups is believed to arise from partial degradation of TMA monomer during plasma surface modification. In addition, the actual ratio N/S presented in Table 1 confirms results of FT-IR: it seems easier to efficiently control a TMA/SA ratio to 1, than to 0.5 or 2, which suggests that excess of negative or positive charge in the initial coating bath cannot lead to the exact targeted grafting, that is PVDF-*g*-T1/S2 and PVDF-*g*-T2/S1, respectively. If TMA is in large excess, we hypothesize that the degradation of quaternary ammonium does not permit to maintain the initial ratio, or the excess of TMA in the initial coating bath is expelled, then preventing an efficient grafting. If SA is in excess, we observed that particulates were formed, and that many SA particles were blown away during the plasma treatment. If TMA and SA are in equal amount in the initial coating bath, it seems that the negative effect of plasma on TMA (partial degradation) is masked by the presence of SA and vice-versa. Nevertheless, the excess of either positive or negative moieties at the interface is still maintained for PVDF-*g*-T2/S1 and PVDF-*g*-T1/S2, respectively. This excess of charges will be noted as charge-bias in the present study. For the sake of ease, we will consider theoretical charge-bias, obtained from the initial molar ratio of TMA and SA, and experimental "true" charge-bias obtained from FT-IR and XPS analysis are given in Table 1. Finally, the measurements of zeta-potential at pH 7.4 presented in Table 1 confirm the results of chemical analysis regarding the charge bias. The membrane modified with an equimolar ratio of TMA and SA presents a zeta potential close to 0 ($\xi = 0.6 \pm 5.2$ mV), but the error limit on data suggests that surface homogeneity could still be improved. Increasing the TMA/SA ratio logically leads to an excess of positive charges held by the surfaces ($\xi = 15.2 \pm 2.4$ eV and $\xi = 22.7 \pm 2.7$ eV for PVDF-*g*-T2S1 and PVDF-*g*-T1S0, respectively), while decreasing this ratio leads to further negative surfaces ($\xi = -3.4 \pm 0.5$ mV and $\xi = -8.4 \pm 1.2$ mV for PVDF-*g*-T1S2 and PVDF-*g*-T0S1, respectively).

3.2. Biofouling mitigation of surface-modified PVDF membranes

3.2.1. Hydration properties of surface-modified PVDF membranes

A generally accepted result is that in order to efficiently resist biofouling, a surface or a porous matrix should be hydrophilic. This concept of fouling-resistance is opposed to that of fouling-release for which hydrophobic interfaces are at play. Here, we designed these membranes in order to resist biofouling. Therefore, they should first favor water entrapment. Hydrophilicity can be

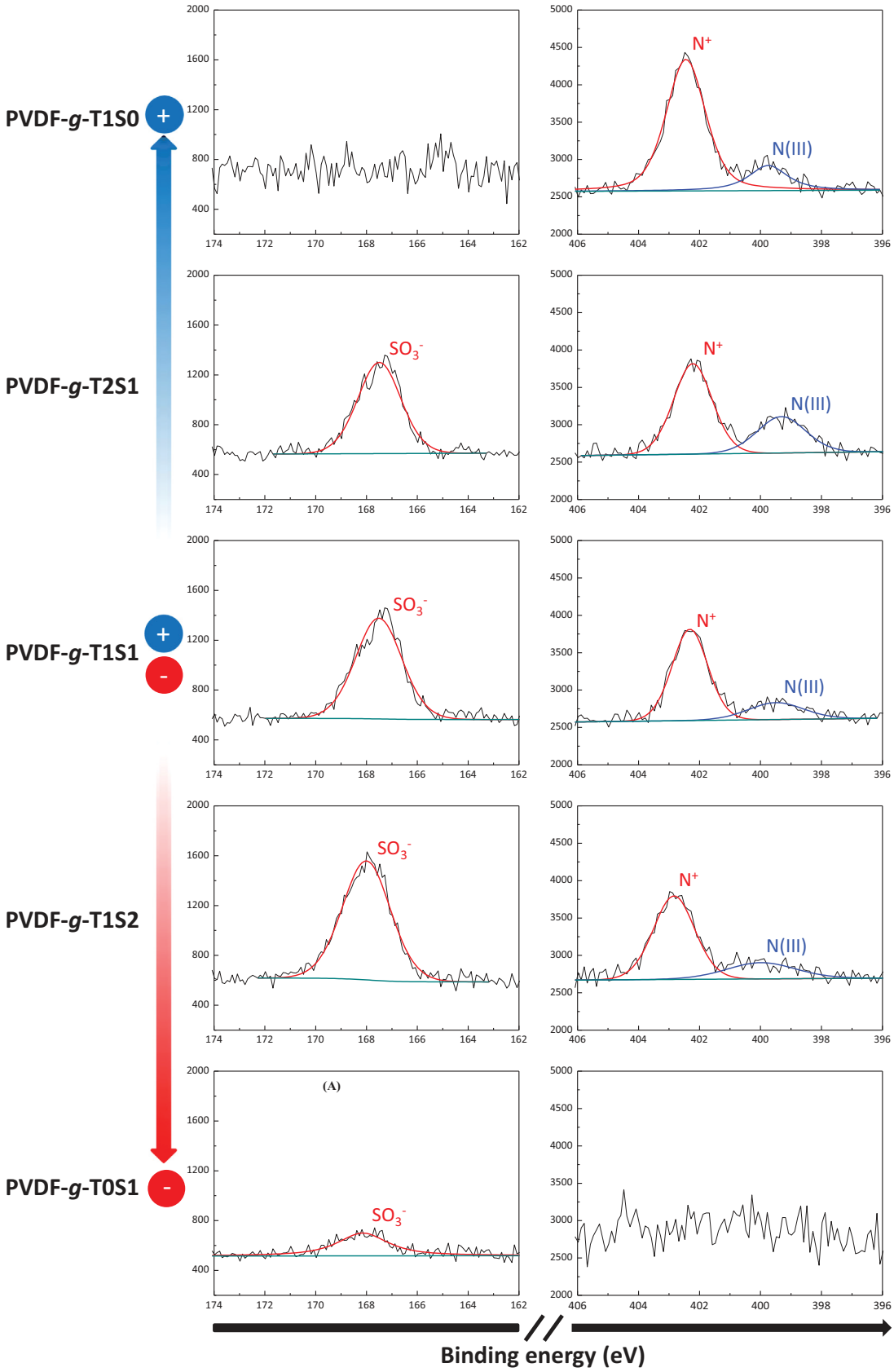

Fig. 5. XPS analysis of virgin and surface-modified membranes.

assessed through the evaluation of water contact angle and hydration capacity (Fig. 6). While the first measurement indicates how hydrophilic the surface is, the second test gives important information on the ability of polymer brushes to trap water. Our result indicate that the water contact angle of virgin membrane is logically very high (113°), resulting from both the hydrophobic

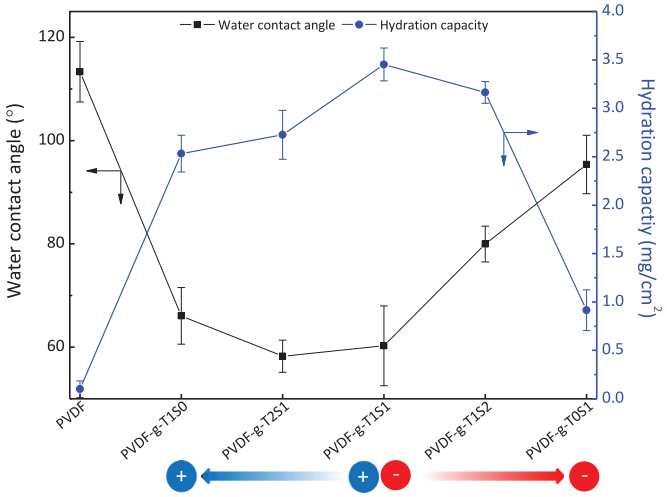

Fig. 6. Effect of plasma surface modification and of mixed-charge molar ratio on hydration properties of grafted layers.

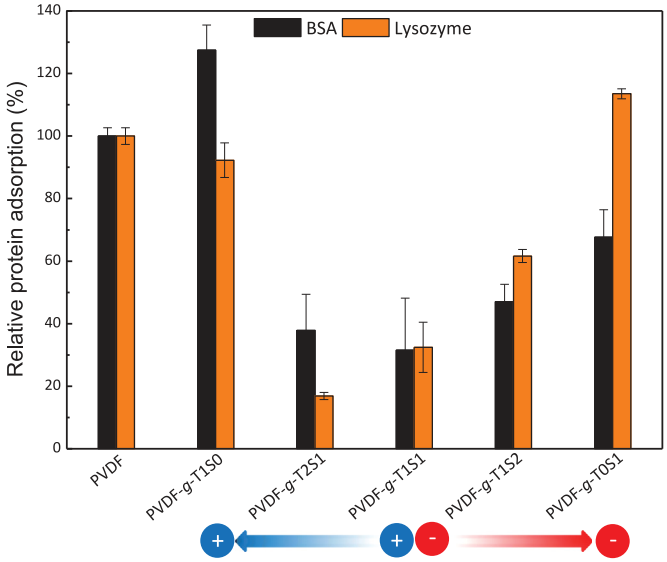

Fig. 7. Effect of surface modification of PVDF membranes and surface charge-bias on resistance to nanofouling by BSA and lysozyme proteins.

nature of the polymer but also from the penalty offered by the porous rough matrix. The physical state of the membrane is clearly not favorable to the formation of a hydrophilic interface. The chemical surface modification highlights that membranes that are positively charged (excess of TMA) or pseudo-zwitterionic (TMA/SA: 1/1) exhibit an important decreasing of water contact angle to reach a plateau around 60°. However, membranes with excess of negative charges are not as hydrophilic since water contact angle of PVDF-*g*-T1S2 and PVDF-*g*-T0S1 are 80° and 95°, respectively. All surface-modified materials contain numerous hydrogen-bond acceptors, which favors H-bond formation with water molecules. However, it appears that hydration behaviors of positive ions and negative ions are different. The explanation might be related to Yang et al. study [30]. Particularly, they pointed in their simulation work the importance of the charge distribution in water in distinguishing the positive and negative charges through different hydration. Additionally, the trend observed for water contact angle is also seen on hydration capability plot, which suggests that water molecules will be trapped more efficiently in the grafted layer of membranes either positively charged or neutral. It implies that in the absence of electrostatic interactions, these membranes should be more efficient to mitigate biofouling.

3.2.2. *Mitigation of biofouling in static conditions*

The extent of biofouling can be evaluated in static conditions by performing protein adsorption tests and bacterial attachment assays (Figs. 7 and 8). A different scale of biofouling is involved in each case as proteins interact with surfaces at the nanoscale while microscale is at play in the case of biofouling by bacterial species. In general, if the ability of membranes to maintain a highly hydrated state is a pre-requisite to biofouling resistance, our results also unveil that this condition alone is not enough as high levels of protein adsorption were observed onto PVDF-*g*-T1S0 despite a high hydration capability (2.5 ± 0.2 mg/cm^2). Surface packing of antifouling moieties, their length and flexibility, along with the surface charge and the surface porosity are also important parameters that should not be overlooked in the control of biofouling. Except for PVDF-*g*-T0S1 that exhibited a low grafted density, also explaining the high level of protein adsorption regardless their nature, packing is about the same for all membranes (Fig. 2). In a first assumption, we will consider that the length and the flexibility of the grafted layers are not the major parameters explaining the results of protein adsorption, because there is no drag force as during filtration. The surface porosity is qualitatively the same for all membranes, from morphological observations (Fig. 3 and S1), and clearly favors biofouling. The charge is a key parameter here, as presented in earlier section. In the conditions of test, performed at neutral pH, lysozyme is positively charged while BSA carries an overall negative charge [31]. This suggests that electrostatic attractive forces should be maximum between positively-charged membranes and BSA on one hand, and negatively-charged membranes and LY on the other hand, leading to important protein adsorption. This was indeed found as PVDF-*g*-T1S0 ($\xi = 22.7 \pm 2.7$ mV) importantly interacted with BSA while maximum LY adsorption was found with PVDF-*g*-T0S1 membranes ($\xi = -8.4 \pm 1.2$ mV). We also suspect that electrostatic interactions alone do not explain nano-biofouling. Otherwise, the extent of LY and BSA adsorption on PVDF-*g*-T1S0 and PVDF-*g*-T0S1, respectively, would not be as high. As above-mentioned, the low grafting density of SA brushes onto PVDF-*g*-T0S1 membrane must have accounted too for high level of BSA protein adsorption. As for the extent of LY adsorption onto PVDF-*g*-T1S0, it can be explained by concomitant effects of heterogeneous adsorption, lack of surface homogeneity and potentially heterogeneous distribution of the charge in the proteins. Wang et al. studied the adsorption of lysozyme on ceria nanoparticles presenting different surface charges [32]. Even though the level of adsorption on the as-synthesized positive ceria nanoparticles was not as high as those measured on neutral and negative surfaces, it was not zero (adsorption capacity at equilibrium up to 180 mg/g). They pointed that adsorption behavior was typical of heterogeneous adsorption. It is influenced not only by the charge of the surface, but also by the orientation of protein, and the lateral effects between adsorbed molecules. Also, local negative domains of the protein may have come into contact with the surface, thus promoting protein adsorption. Furthermore, if the surface modification is not perfectly homogeneous, then some proteins have probably managed to approach the porous surface and adsorb on it. Finally, lowest adsorption levels were found for pseudo-zwitterionic membranes and membranes with a slight actual excess of positive and negative charges. The pseudo-zwitterionic membranes, meet the Whitesides criteria [16] and therefore exhibit very low-biofouling. For the membranes with an excess of positive or negative charges, we found from FT-IR and XPS analysis, that the excess of charge was not as important as that expected from calculation of monomer ratio in the coating bath. Therefore, the charge-bias was not as high as expected (also confirmed by measurements of zeta potentials). This, combined to

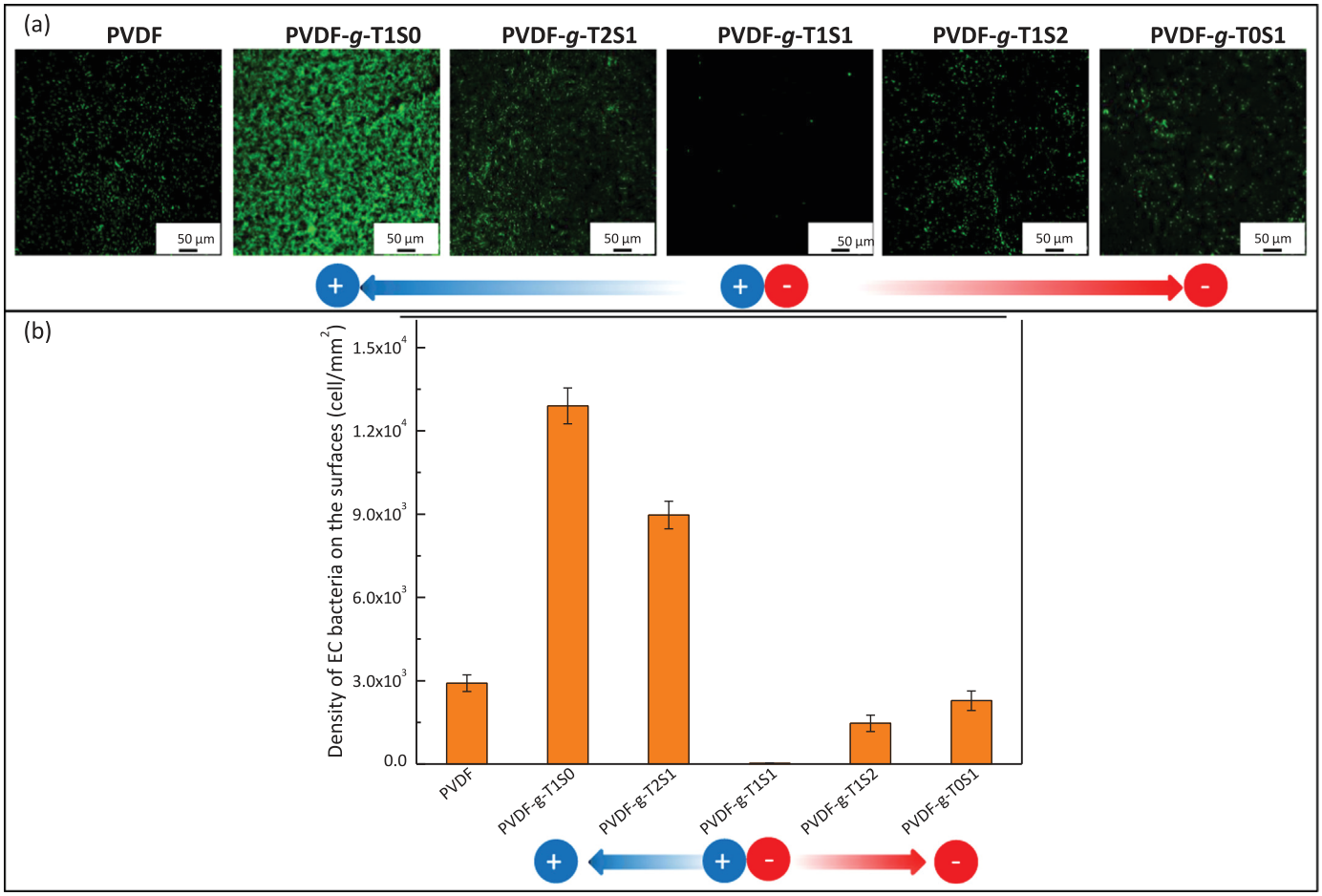

Fig. 8. Resistance of surface-modified membranes to the adhesion of *Escherichia coli*. (a) confocal observations of surfaces; (b) quantitative attachment obtained from the analysis of confocal images.

high hydration of samples, eventually explained the quite low level of protein adsorption. One could expect that actual TMA/SA ratio of 2:1 and 1:2 would lead to higher adsorption levels.

Bacteria found in waters are another major cause of biofouling. To mimic this biofouling and evaluate the ability of grafted layers to repel bacterial species, we carried out adsorption tests, using *Escherichia coli* as a model bacterium. Results of this test are presented in Fig. 8(a) showing confocal observation of biofouling, and in Fig. 8(b) displaying the related quantitative analysis. Our results indicate that PVDF membrane importantly interacts with bacteria, because of concomitant hydrophobic nature and high surface porosity. However, more bacteria adsorbed on positively charged membranes PVDF-*g*-T1S0 and PVDF-*g*-T2S1, which was explained by the electrostatic interactions occurring between the surfaces and the negatively charged cell wall of *E. coli*. So, one could have expected that repulsive electric forces between negative surfaces and cell walls would favor repellence of bacteria. But like for protein adsorption test results, the poor surface grafting density obtained for PVDF-*g*-T0S1 membranes explains the important extent of E. coli adsorption. However, the anti-bacterial attachment properties of pseudo-zwitterionic membranes, compete with some of the best recent surface-modified antifouling PVDF membranes, whether grafted with HEMA-derivatives [8] or containing antifouling nanoparticles [33], as extremely low level of bacterial attachment could be visualized and quantified. This further supports the efficiency of pseudo-zwitterionic brushes, and their ability to replace existing nonfouling materials, or at least to offer appropriate alternates which would not lose their nonfouling nature in harsh environment, like PEG, or if combined with other brushes like some zwitterionic polymers.

3.2.3. *Mitigation of biofouling in dynamic conditions*

Previous section highlighted that resistance to biofouling in static conditions strongly depended on the ratio of mixed-charge which actually permits to control (i) the quality of surface grafting, (ii) the extent of hydration and (iii) the surface charge. Protein adsorption was clearly reduced on non-charged surfaces or surfaces with a low charge bias, while bacterial attachment in the conditions of the test (negative cell-wall) requires a pseudo-zwitterionic or a negatively charged surface. But these tests did not involve any drag force at all. In other words, biofoulants were not pushed toward the membranes and forced to penetrate within the brushes, as in actual conditions of filtration. Yet, polymers resisting compression should be used in the design of nonfouling surfaces because flexibility and chain length are key parameters to consider. In the absence of reliable data on brush thickness and brush mechanical properties that would indicate whether the as-prepared surfaces actually resist biofouling in dynamic conditions, we ran filtration test in standard conditions (1 atm TMP and ambient temperature) using 1 g/L BSA solutions. We tested the pristine membrane, and the pseudo-zwitterionic membrane PVDF-*g*-T1S1, and ran water-BSA filtration cycles, as presented in Fig. 9.

We first noticed that water permeability of virgin and PVDF-*g*-T1S1 membranes was about the same, around 1200 kg/m^2 h, which indicates that surface modification has not led to partial pore blockage, as qualitatively seen from SEM images (Fig. 3) and earlier mentioned.

We observed that the water permeability of PVDF membranes

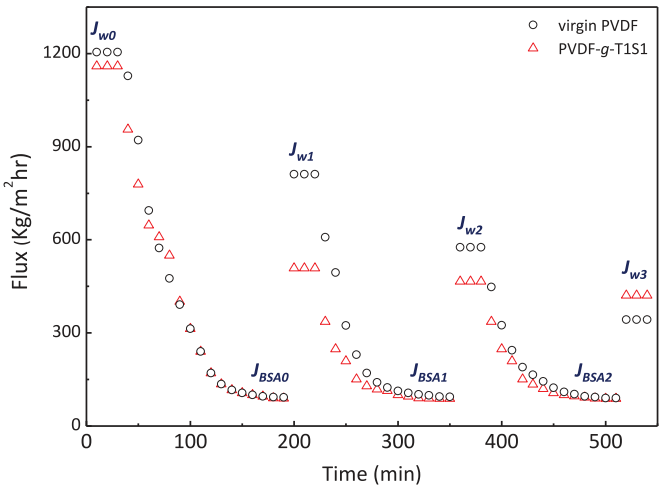

Fig. 9. Resistance of membranes to biofouling by BSA protein during filtration.

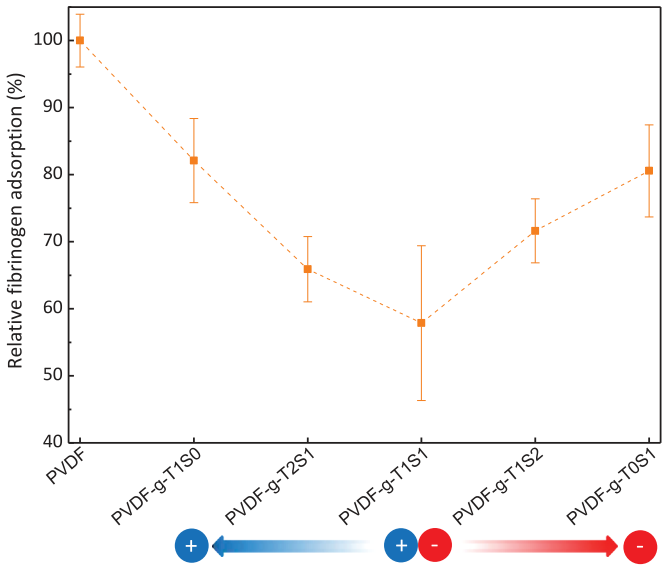

Fig. 10. Resistance of virgin and surface-modified membranes to fibrinogen adsorption.

gradually decreased (Fig. 9), and the flux recovery ratio after each cycle was always in the range 60–70% (Table 2), which indicated that sites were gradually fouled by BSA. As for the grafted sample, we suspected that a lack of surface uniformity was responsible for the low flux recovery measured after the first cycle (FRR=44% after cycle 1). The technique used here involved no preliminary activation of the surface. After coating, activation and grafting were done all at once. Plasma-induced post grafting and plasma polymerization happened concomitantly and may have led to a partial lack of surface and bulk homogeneity. Therefore, rather important biofouling occurred after the first cycle. However, if the method can be improved, the chemical efficiency of TMA and SA (1:1) is clearly seen during cycles 2 and 3, as very high FRR are then obtained (92% and 89%, respectively). It implies that no subsequent fouling occurred. In other words, all sites that could potentially be fouled were fouled during the first cycle, and corresponded to all unmodified sites of the porous membranes due to surface heterogeneities. So, the efficiency of mixed-charges in dynamic conditions is proven here, even if further efforts are needed to improve the surface homogeneity of the pseudo-zwitterionic membrane. Eventually, membrane modified with the pseudo-zwitterionic moieties presents higher global flux recovery ratio, lower irreversible flux decline ratio and higher reversible flux decline ratio than virgin PVDF membrane (Table 2), revealing the positive effect of TMA/SA brushes on mitigation of biofouling in dynamic conditions.

3.3. *Hemocompatibility of surface-modified PVDF membranes*

Resistance to biofouling is a requirement not only for membranes applied in water treatment related applications, but also for those applied in blood-contacting devices. There has been much less investigations carried out on the design of hemocompatible porous membranes than on membranes for water treatment. Yet, both types of membranes have similar requirements, and it would not be surprising that effective designs for water treatment could be applied in blood filtration. In addition, versatile designs permit to improve the cost-efficiency of membrane production. Therefore, we performed a number of tests oriented toward the evaluation of hemocompatibility of these surface-modified membranes.

A first important test concerns the evaluation of the resistance to the adsorption of fibrinogen, a plasma protein mediating platelet adhesion and activation [34]. Alike for other proteins investigated in Section 3.2.2, good packing of antifouling moieties should be reached in order to prevent nano-biofouling by this protein. Results of Fig. 10 indicate that PVDF is severely fouled by this very sticky protein, eventually exhibiting the highest relative protein adsorption. PVDF-g-T1S0 and PVDF-g-T2S1 membranes have a positive charge-bias, and so, establish electrostatic interactions with FN which is negatively charged at physiological pH [35,36]. The slightly lower adsorption of fibrinogen than that measured on virgin PVDF membrane is ascribed to the quite important hydration of these membranes. As the charge bias decreases (from PVDF-g-T1S0 to PVDF-g-T1S1), interactions between the membranes and fibrinogen are reduced to the minimum level observed in this study, indicating the low-biofouling nature of pseudo-zwitterionic membranes, with respect to this particular protein. It is important to stress on the fact that the plateau reached at 60% could probably be lowered, provided an improvement of the surface homogeneity after plasma modification process. Indeed, the efficiency of the TMA/SA couple to resist the

Table 2
Flux analyses.

Sample ID	Flux recovery ratio (%)*				Reversible flux decline ratio (%)*				Irreversible flux decline ratio (%)*			
	$FRR = (J_{wi}/J_{wi-1})\times 100$				$DR_r = [(J_{wi} - J_{BSAi})/J_{wi-1}]\times 100$				$DR_{ir} = [(J_{wi-1} - J_{wi})/J_{wi-1}]\times 100$			
	Cycle 1 $i=1$	Cycle 2 $i=2$	Cycle 3 $i=3$	GLOBAL	Cycle 1 $i=1$	Cycle 2 $i=2$	Cycle 3 $i=3$	GLOBAL	Cycle 1 $i=1$	Cycle 2 $i=2$	Cycle 3 $i=3$	GLOBAL
PVDF	68	71	59	28	60	60	43	21	33	29	42	72
PVDF-g-T1S1	44	92	89	36	36	75	71	29	56	8	11	64

* The global flux recovery ratio, the global reversible flux decline ratio and the global irreversible flux decline ratio were calculated by considering the initial water flux J_{w0}, the final water flux J_{w3}, and the very last BSA flux J_{BSA2} in the related equations.

adsorption of FN onto modified ePTFE surfaces was earlier proven with a level reduced to 40% the limitation of virgin ePTFE membranes [23], which supports the need for an improvement of the control of the modification process. We also observed that membranes negatively charged still interacted with the protein, which suggests that the adsorption of FN occurred against the repulsive electrostatic forces. Such a phenomenon was reported earlier by Marucco et al. [35], who studied the interaction of FN with TiO_2 nanoparticles, presenting a negative surface charge. They explained that charge distribution in FN protein is heterogeneous. Based on Jung et al. work [37], they explained that the αC regions of FN, positively charged, eventually enabled the orientation of the protein and facilitated its adsorption. For PVDF-*g*-T0S1, a poor-packing of charged brushes associated with very low level of hydration must be responsible for the high level of adsorption.

We then moved onto the assessment of platelet adhesion tests. Confocal images presented in Fig. 12 clearly show that positive surfaces importantly interact with platelets. Adsorption of platelets was also seen on virgin PVDF membranes, while pseudo-zwitterionic membrane (PVDF-*g*-T1S1) and negatively-charged membranes (PVDF-*g*-T1S2 and PVDF-*g*-T0S1) did not interact with platelets at all. Therefore, if resistance to fibrinogen is important, the surface electric charge of the membrane plays a key role. As the cell-wall of platelets is negatively charged [38], interactions occur with PVDF-*g*-T1S0 and PVDF-*g*-T2S1. As for PVDF membrane, they also interact with platelet because of their hydrophobic nature and high porosity, and following a similar mechanism as that of bacterial attachment. Also, if FN alone explained the adhesion of platelets, then more cells should have been observed on virgin PVDF membranes, which means that the charge of the interface is probably more important. Logically, membranes with a negative charge bias did not (or slightly) interact with platelets.

We then studied the adsorption of red blood cells by confocal microscopy. The confocal images of red blood cell adsorption and quantitative analysis associated, also presented in Fig. 11, evidence quite similar results to those observed for platelet adhesion, that is, numerous cells could be observed onto and within virgin PVDF and positively-charged membranes, while no cell was observed on

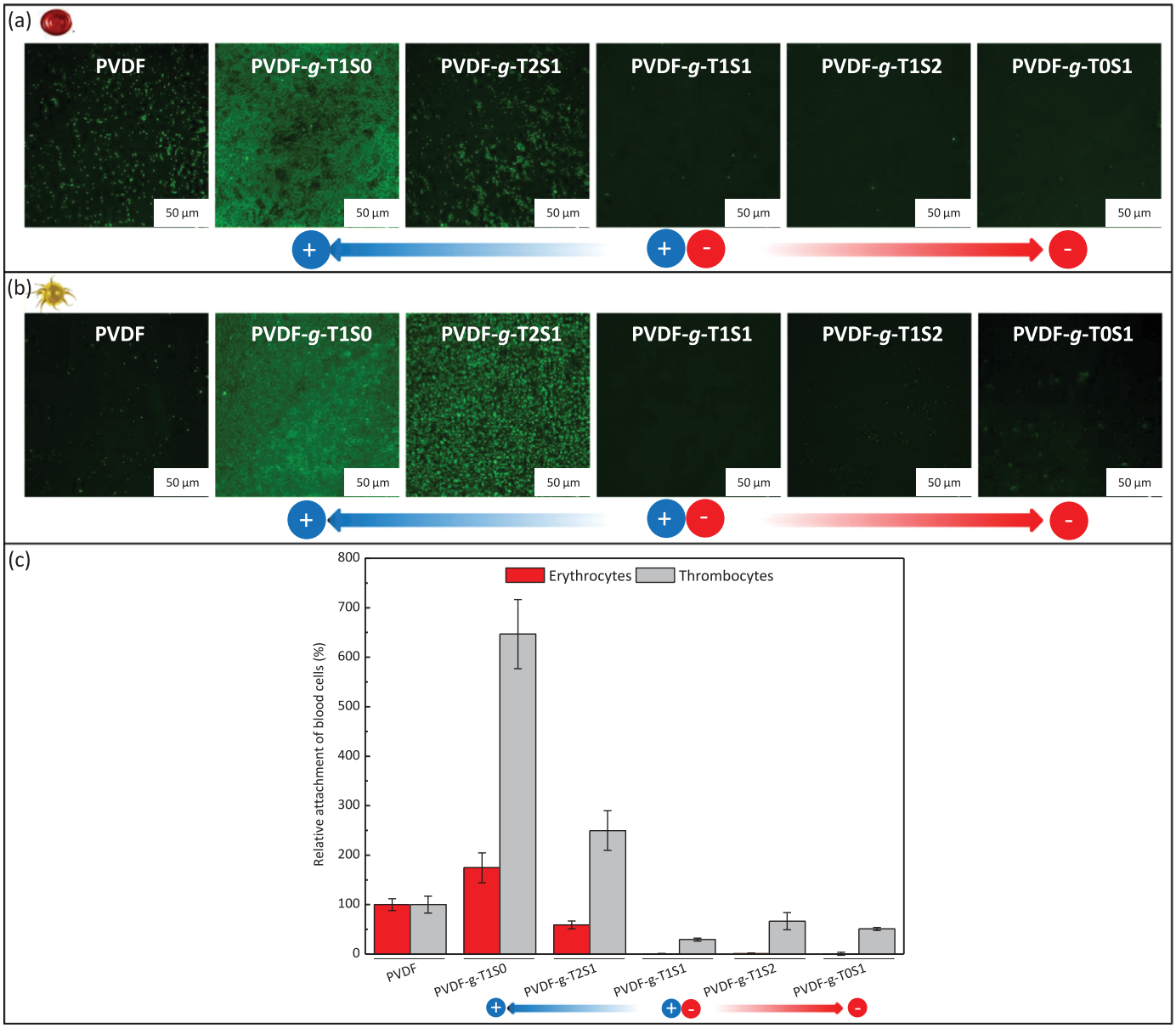

Fig. 11. Effect of surface modification and charge-bias on the adhesion of (a) erythrocytes and (b) thrombocytes. The bottom panel (c) represents the related quantification of blood cells adhering onto the surfaces obtained from the analysis of confocal images.

Table 3
Hemolytic activity of membranes.

Sample ID	Hemolysis ratio (%)
PVDF	0.26 ± 0.16
PVDF-*g*-T1S0	1.85 ± 0.16
PVDF-*g*-T2S1	0.53 ± 0.30
PVDF-*g*-T1S1	0.42 ± 0.10
PVDF-*g*-T1S2	0.15 ± 0.05
PVDF-*g*-T0S1	0.11 ± 0.05

the images of pseudo-zwitterionic and negatively charged membranes. Alike for other biofoulants, the physicochemical nature of PVDF membranes can explain their important level of interaction with RBCs. However, another parameter is believed to favor the adsorption and penetration of RBCs in the membrane: their deformability. RBCs can penetrate within capillaries of the vascular system whose diameter is significantly smaller than that of the cells, to supply all the body tissues with oxygen. Following a similar mechanism, it is believed that the deformability of RBCs could allow them to penetrate in smaller pore than their diameter. The positive charge held by PVDF-*g*-T1S0 and PVDF-*g*-T2S1 also favors the interactions with the negatively charged cell wall of the membrane. Indeed, literature mentions that positively charged chitooligosaccharides interact with the red blood cells, and more specifically with the negatively charged sialic acids [39]. Notice that interactions of positively charged surfaces with RBCs were also reported by Han et al. [40]. Finally, we tested the hemolytic activity of membranes (Table 3). The acceptable hemolysis for a material to be considered as biocompatible is 5%. Referring to this value, all membranes of this study could be considered as potentially biocompatible. However, Zhao et al. reminded us that the lack of hemolytic activity does not warrant the absence of interactions between the surface considered, here the PVDF membrane, and the blood cells [41]. It is also important to keep in mind that in this test, cells are not stressed by the action of blood flow leading to frictions with material interfaces alike in blood filtration devices. Therefore, it is essential to keep a very low value of hemolysis as the extent of cell lysis in real application is expected to be higher. Nonetheless, the highest hemolytic activity value is obtained with positively charged membranes, with is consistent with results of RBCs attachment, as a positive charge promotes the adhesion of cells.

3.4. Remarks on the efficiency of GDBD plasma grafting to reach membrane nonfouling

The chemical efficiency of TMA/SA mixed-charge polymer brushes (chemical effect) to resist biofouling of PVDF MF membranes has been evidenced. However, previous sections all unveiled that if biofouling was importantly mitigated in static conditions, it could be further reduced or totally inhibited in dynamic conditions. To improve performances of TMA/SA grafted PVDF membranes and achieve nonfouling, the focus of the debate should be placed on the methods to increase the grafting density (physical effect) in order to block all potential adsorption sites to biofoulants. The efficiency of the grafting method depends on the material matrix itself (especially pore size distribution of the PVDF membrane) and on the plasma treatment. As PVDF membranes were commercial ones, we lay the focus on the plasma modification process that we conducted and propose some directions to improve it in subsequent investigations.

The process used is a hand-made glow dielectric barrier discharge (GDBD) type of plasma treatment (Fig. 12). In discharge process, surface-modification is carried out inside the plasma discharge [42]. Thus, modification is faster than with downstream

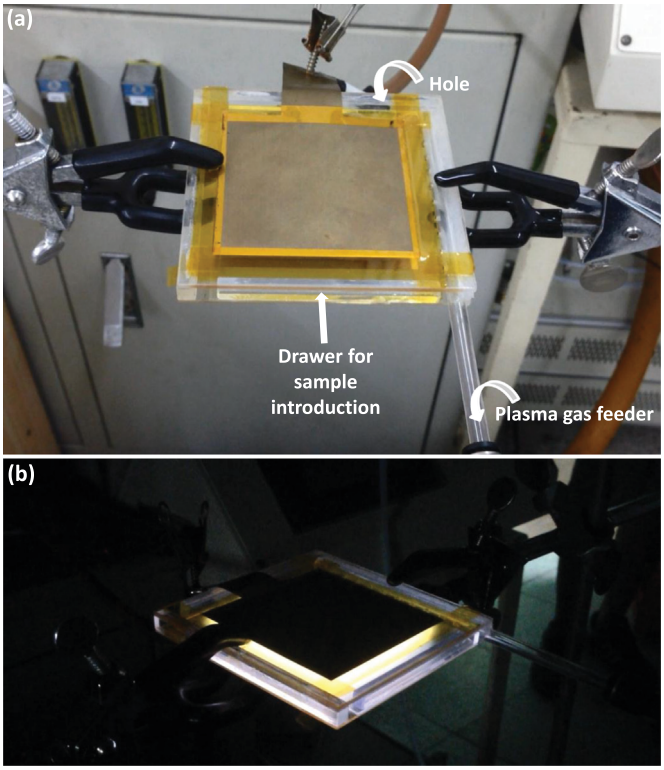

Fig. 12. Hand-made glow dielectric barrier discharge plasma treatment. The plasma gas tube feeder and the hole for cooling and air circulation highlighted in (a) are believed to be key engineered parts to optimize in order to improve the final surface homogeneity of surface-modified membranes; (b) Process in operation.

processes using one single jet or line source [43], for which surface modification is made outside the plasma discharge, by scanning back and forth the surface. However, one major advantage of downstream processes is that they lead to optimized surface homogeneity, which suggests that a complete change of cell configuration could permit to better mitigate fouling of grafted membranes by improving the distribution of TMA/SA brushes over the surface. In addition, downstream processes allow treating homogeneously large surfaces, which should be considered in case of potential scale-up. Therefore, a way to go would be to switch from discharge to downstream configuration.

Nevertheless, if one wants to keep a similar GDBD cell configuration, efforts must be done on the flow distribution of plasma gas as the homogeneity of final surfaces strongly depend on the circulation pattern of plasma gas. In our configuration, a tube disposed between the dielectric barriers serves both as a spacer and as a plasma gas feeder. Although holes in the tube wall were carefully engineered and regularly spaced to enable homogeneous distribution of gas transfer, complementary tests could be run to determine the optimal configuration leading to improved flow pattern of gas inlet, and so to a better homogeneity of surface. We suspect that both the number and the size of these gas feeding holes play important roles. Additionally, space was left empty in the wall opposite to that from which the sample was introduced in the chamber, enabling both to promote convection inside the chamber and to cool down the system by air introduction. The position of this empty space as well as its surface area may play a key role too, and should be the object of a dedicated study. Given the number of parameters potentially influencing the temperature and the flow pattern and eventually the surface homogeneity of grafted membranes and their efficiency to resist fouling in dynamic condition, an experimental design could be run, using FRR after the 1st water-BSA cycle as dependent variable. By doing so,

one could clearly optimize the GDBD chamber and fully take advantage of both the speed of the process and of the great chemical potential of TMA/SA mixed-charge as surface-modifier for the design of nonfouling PVDF membranes.

4. Conclusion

In this work, we have presented a novel antifouling pseudo-zwitterionic PVDF membrane, using the surface grafting of TMA/SA mixed-charge copolymer via GDBD plasma-induced surface copolymerization. One can fairly control the surface charge of the membrane, through the initial molar content, and prepare either pseudo-zwitterionic membranes, or membranes with a positive or a negative charge bias. The aim was to test the feasibility of the process and investigate the low-biofouling properties of the membranes, with respect to biofoulants found in water or in blood, to broaden the range of application of these membranes.

Overall, pseudo-zwitterionic membranes exhibit excellent resistance to biofouling in static conditions. Hence, surface-modified membranes resist protein adsorption, ascribed to the nonfouling power of mixed-charges or to electrostatic repulsions when a charge bias was involved. In a same manner, biofouling by *Escherichia coli* was mitigated, as well as that by blood cells (platelets and erythrocytes).

Nonetheless, we still observed an important decrease of flux recovery after the 1st cycle of a standard water/protein filtration, which clearly highlighted that some sites of the membrane were fouled. After 2nd and 3rd cycle, very high FRR evidenced again the chemical efficiency of TMA/SA to resist biofouling. We found that despite an excellent chemical effect of TMA/SA on fouling resistance, surface coverage (physical effect) of mixed-charge must be improved to inhibit fouling from the very first cycle, which could be doable by optimizing the flow pattern in the GDBD process employed. By comparison, the virgin PVDF membrane was gradually fouled and FRR kept on decreasing.

Therefore, this combination of results provide the original evidence that pseudo-zwitterionic PVDF membranes can be applied in either water treatment or blood filtration, even if some efforts still need to be done to improve the surface grafting density and homogeneity, by carefully tuning the process parameters. This is the object of on-going studies.

Acknowledgments

The authors would like to acknowledge the project of Outstanding Professor Research Program in the Chung Yuan Christian University, Taiwan (11757) and the Ministry of Science and Technology (MOST 102-2923-E-033-001-MY3, 103-2221-E-033-078-MY3, and 103-2622-E-033-007-CC1) and to the 2013–2015 NSC-ANR Blanc International II Program (Taiwan–France Project: SuperNAM, ANR-12-IS08-0002) for their financial support. The authors would like to extend their sincere appreciation to the Deanship of Scientific Research at King Saud University for its funding of this research through the Research Group Number (RG-1435-081).

References

[1] Q. Shi, Y. Su, S. Zhu, C. Li, Y. Zhao, Z. Jiang, A facile method for synthesis of pegylated polyethersulfone and its application in fabrication of antifouling ultrafiltration membrane, J. Membr. Sci. 303 (2007) 204–212.
[2] Y. Su, C. Li, W. Zhao, Q. Shi, H. Wang, Z. Jiang, S. Zhu, Modification of polyethersulfone ultrafiltration membranes with phosphorylcholine copolymer can remarkably improve the antifouling and permeation properties, J. Membr. Sci. 322 (2008) 171–177.
[3] H. Qin, C. Sun, C. He, D. Wang, C. Cheng, S. Nie, S. Sun, C. Zhao, High efficient protocol for the modification of polyethersulfone membranes with anticoagulant and antifouling properties via in situ cross-linked copolymerization, J. Membr. Sci. 468 (2014) 172–183.
[4] X. Fan, Y. Su, X. Zhao, Y. Li, R. Zhang, J. Zhao, Z. Jiang, J. Zhu, Y. Ma, Y. Liu, Fabrication of polyvinyl chloride ultrafiltration membranes with stable antifouling property by exploring the pore formation and surface modification capabilities of polyvinyl formal, J. Membr. Sci. 464 (2014) 100–109.
[5] D.G. Kim, H. Kang, S. Han, J.C. Lee, The increase of antifouling properties of ultrafiltration membrane coated by star-shaped polymers, J. Mater. Chem. 22 (2012) 8654–8661.
[6] A. Venault, Y. Chang, H.S. Yang, P.Y. Lin, Y.J. Shih, A. Higuchi, Surface self-assembled zwitterionization of poly(vinylidene fluoride) microfiltration membranes via hydrophobic-driven coating for improved blood compatibility, J. Membr. Sci. 454 (2014) 253–263.
[7] H.Y. Yu, L.Q. Liu, Z.Q. Tang, M.G. Yan, J.S. Gu, X.W. Wei, Surface modification of polypropylene microporous membrane to improve its antifouling characteristics in an SMBR: air plasma treatment, J. Membr. Sci. 311 (2008) 216–224.
[8] Y. Sui, X. Gao, Z. Wang, C. Gao, Antifouling and antibacterial improvement of surface-functionalized poly(vinylidene fluoride) membrane prepared via dihydroxyphenylalanine-initiated atom transfer radical graft polymerizations, J. Membr. Sci. 394–395 (2012) 107–109.
[9] W.W. Yue, H.J. Li, T. Xiang, H. Qin, S.D. Sun, C.S. Zhao, Grafting of zwitterion from polysulfone membrane via surface-initiated ATRP with enhanced antifouling property and biocompatibility, J. Membr. Sci. 446 (2013) 79–91.
[10] A. Maartens, E.P. Jacobs, P. Swart, UF of pulp and paper effluent: membrane fouling-prevention and cleaning, J. Membr. Sci. 209 (2002) 81–92.
[11] A.C. Sagle, E.M. Van Wagner, H. Ju, B.D. McCloskey, B.D. Freeman, M. M. Sharma, PEG-coated reverse osmosis membranes: Desalination properties and fouling resistance, J. Membr. Sci. 340 (2009) 92–108.
[12] R.M. Gol, A. Bera, S. Banjo, B. Ganguly, S.K. Jewrajka, Effect of amine spacer of PEG on the properties, performance and antifouling behavior of poly(piperazineamide) thin film composite nanofiltration membranes prepared by in situ PEGylation approach, J. Membr. Sci. 472 (2014) 154–166.
[13] Z. Yi, L.P. Zhu, Y.Y. Xu, X.N. Gong, B.K. Zhu, Surface zwitterionicalization of poly (vinylidene fluoride) porous membranes by post-reaction of the amphiphilic precursor, J. Membr. Sci. 385–386 (2011) 57–66.
[14] M.L. Li, J.H. Li, X.S. Shao, J. Ming, J.B. Wang, Q.Q. Zhang, X.P. Xu, Grafting zwitterionic brush on the surface of PVDF membrane using physisorbed free radical grafting technique, J. Membr. Sci. 405–406 (2012) 141–148.
[15] Q. Zhou, X.P. Lei, J.H. Li, B.F. Yan, Q.Q. Zhang, Antifouling, adsorption and reversible flux properties of zwitterionic grafted PVDF membrane prepared via physisorbed free radical polymerization, Desalination 337 (2014) 6–15.
[16] R.G. Chapman, E. Ostuni, S. Takayama, R.E. Holmlin, L. Yan, G.M. Whitesides, Surveying for surfaces that resist the adsorption of proteins, J. Am. Chem. Soc. 122 (2000) 8303–8304.
[17] S. Chen, F. Yu, Q. Yu, Y. He, S. Jiang, Strong resistance of a thin crystalline layer of balanced charged groups to protein adsorption, Langmuir 22 (2006) 8186–8191.
[18] S. Chen, S. Jiang, A New avenue to nonfouling materials, Adv. Mater. 20 (2008) 335–338.
[19] Y. Chang, S.H. Shu, Y.J. Shih, C.W. Chu, R.C. Ruaan, W.Y. Chen, Hemocompatible mixed-charge copolymer brushes of pseudozwitterionic surfaces resistant to nonspecific plasma protein fouling, Langmuir 26 (2010) 3522–3530.
[20] L. Mi, M.T. Bernards, G. Cheng, Q. Yu, S. Jiang, pH responsive properties of nonfouling mixed-charge polymer brushes based on quaternary amine and carboxylic acid monomers, Biomaterials 31 (2010) 2919–2925.
[21] S.C. Dobbins, D.E. McGrath, M.T. Bernards, Nonfouling hydrogels formed from charged monomer subunits, J. Phys. Chem. B 116 (2012) 14346–14352.
[22] M.E. Schroeder, K.M. Zurick, D.E. McGrath, M.T. Bernards, Multifunctional polyampholyte hydrogels with fouling resistance and protein conjugation capacity, Biomacromolecules 14 (2013) 3112–3122.
[23] J.F. Jhong, A. Venault, L. Liu, J. Zheng, S.H. Chen, A. Higuchi, J. Huang, Y. Chang, Introducing mixed-charge copolymers as wound dressing biomaterials, ACS Appl. Mater. Interfaces 6 (2014) 9858–9870.
[24] Y.H. Zhao, X.Y. Zhu, K.H. Wee, R. Bai, Achieving highly effective non-biofouling performance for polypropylene membranes modified by UV-induced surface graft polymerization of two oppositely charged monomers, J. Phys. Chem. B 114 (2010) 2422–2429.
[25] Y. Chang, Y.J. Shih, C.Y. Ko, J.F. Jhong, Y.L. Liu, T.C. Wei, Hemocompatibility of poly(vinylidene fluoride) membrane grafted with network-like and brush-like antifouling layer controlled via plasma-induced surface PEGylation, Langmuir 27 (2011) 5445–5455.
[26] Q. Li, Q.Y. Bi, B. Zhou, X.L. Wang, Zwitterionic sulfobetaine-grafted poly(vinylidenefluoride) membrane surface with stably anti-protein-fouling performance via a two-step surface polymerization, Appl. Surf. Sci. 258 (2012) 4707–4717.
[27] J. Ju, T. Wang, Q. Wang, Superhydrophilic and underwater superoleophobic PVDF membranes via plasma-induced surface PEGDA for effective separation of oil-in-water emulsions, Colloids Surf., A 481 (2015) 151–157.

[28] R. Yang, K.K. Gleason, Ultrathin antifouling coatings with stable surface zwitterionic functionality by initiated chemical vapor deposition (iCVD), Langmuir 28 (2012) 12266–12274.
[29] R. Yang, H. Jang, R. Stocker, K.K. Gleason, Synergistic prevention of biofouling in seawater desalination by zwitterionic surfaces and low-level chlorination, Adv. Mater. 26 (2014) 1711–1718.
[30] L. Yang, Y. Fan, Y.Q. Gao, Differences of cations and anions: their hydration, surface adsorption, and impact on water dynamics, J. Phys. Chem. B 115 (2011) 12456–12465.
[31] K. Rezwan, L.P. Meier, L.J. Gauckler, Lysozyme and bovine serum albumin adsorption on uncoated silica and AlOOH-coated silica particles: the influence of positively and negatively charged oxide surface coatings, Biomaterials 26 (2005) 4351–4357.
[32] B. Wang, P. Wu, R.A. Yokel, E.A. Grulke, Influence of surface charge on lysozyme adsorption to ceria nanoparticles, Appl. Surf. Sci. 258 (2012) 5332–5341.
[33] A. Rahimpour, M. Jahanshahi, B. Rajaeian, M. Rahimnejad, TiO_2 entrapped nano-composite PVDF/SPES membranes: preparation, characterization, antifouling and antibacterial properties, Desalination 278 (2011) 343–353.
[34] T. Beugeling, The interaction of polymer surfaces with blood, J. Polym. Sci. Polym. Symp. 66 (1979) 419–426.
[35] A. Marucco, I. Fenoglio, F. Turci, B. Fubini, Interaction of fibrinogen and albumin with titanium dioxide nanoparticles of different crystalline phases, J. Phys.: Conf. Ser. 429 (2013) 012014.
[36] M. Brust, O. Aouane, M. Thiébaud, D. Flormann, C. Verdier, L. Kaestner, M. W. Laschke, H. Selmi, A. Benyoussef, T. Podgorski, G. Coupier, C. Misbah, C. Wagner, The plasma protein fibrinogen stabilizes clusters of red blood cells in microcapillary flows, Sci. Rep. 4 (2014) 4348.
[37] S.Y. Jung, S.M. Lim, F. Albertorio, G. Kim, M.C. Gurau, R.D. Yang, M.A. Holden, P. S. Cremer, The vroman effect: a molecular level description of fibrinogen displacement, J. Am. Chem. Soc. 125 (2003) 12782–12786.
[38] V. Karagkiozaki, S. Logothetidis, S. Lousinian, G. Giannoglou, Impact of surface electric properties of carbon-based thin fi lms on platelets activation for nanomedical and nano-sensing applications, Int. J. Nanomed. 3 (2008) 461–469.
[39] J.C. Fernandes, P. Eaton, H. Nascimento, L. Belo, S. Rocha, R. Vitorino, F. Amado, J. Gomes, A. Santos-Silva, M.E. Pintado, F.X. Malcata, Effects of chitooligosaccharides on human red blood cell morphology and membrane protein structure, Biomacromolecules 9 (2008) 3346–3352.
[40] Y. Han, X. Wang, H. Dai, S. Li, Nanosize and surface charge effects of hydroxyapatite nanoparticles on red blood cell suspensions, ACS Appl. Mater. Interfaces 4 (2012) 4616–4622.
[41] Y. Zhao, X. Sun, G. Zhang, B.G. Trewyn, I.I. Slowing, V.S.Y. Lin, Interaction of mesoporous silica nanoparticles with human red blood cell membranes: size and surface effects, ACS Nano 5 (2011) 1366–1375.
[42] D. Pappas, Status and potential of atmospheric plasma processing of materials, J. Vac. Sci. Technol. A 29 (2011) 020801.
[43] M. Laroussi, T. Akan, Arc-free atmospheric pressure cold plasma jets: a review, Plasma Process. Polym. 4 (2007) 777–788.